Benchmark Study of The Exchange-Corrected Density Functionals: Application to Strained Boron Nitride Clusters

N.V. Novikov [a], I.Y. Dolinskiy [a], M.A. Gimaldinova [a], K.P. Katin [a,b,1], M.M. Maslov [a,b]

[a] Department of Condensed Matter Physics, National Research Nuclear University MEPhI,

Kashirskoe Sh. 31, Moscow 115409, Russia

[b] Laboratory of Computational Design of Nanostructures, Nanodevices and Nanotechnologies,

Research Institute for the Development of Scientific and Educational Potential of Youth,

Aviatorov Str. 14/55, Moscow 119620, Russia

Abstract: We present a quantum chemical study of three small boron nitride clusters B_2N_2, B_3N_3 and B_4N_4. Their structure and electronic characteristics are calculated by means of the coupled cluster (CC) and density functional theory (DFT) techniques. In order to find the best match with the coupled cluster data the twenty-four DFT exchange-corrected functionals are analyzed. According to our results, B3P86V5 and B97 functionals reproduce well the geometry of small boron-nitrides, whereas for the electronic characteristics OP and VWN functionals give the closest to CC results. Note that prevalent B3LYP and PBE0 DFT-functionals demonstrate lower accuracy.

Keywords: *coupled cluster, density functional theory, exchange-corrected functionals, boron nitride clusters, boron nitride cubane.*

1. Introduction

After discoveries of fullerenes, nanotubes and graphene, many novel carbon architectures were proposed and investigated. They include peapods [1], fullerites [2], diamonds [3,4], and many others [5-8]. In these structures, carbon atoms form k-membered cycles, in which k value varies mostly from 4 to 8. Note, that only a limited number of high-strained structures contains triangle cycles with k = 3 (for example, tetrahedrane derivatives [9-10] and Ladenburg's benzene [11]). The values of k = 4÷8 are prevalent, because it provides more energetically favorable valence angles. Larger cycles with k > 8 often tend to split into two smaller ones via forming of additional carbon-carbon bond between the opposite atoms.

The square cycles (k = 4) are quite strain. The angle between C-C bonds of about 90º is far from the typical values of 109.5º (as in diamond) or 120º (as in graphite). Nevertheless, a number of structures with the square cycles were found to be stable, for example, cubane [12-13] and its derivatives [14-16], prismanes [17] and hypercubane [18]. Moreover, some "non-classical" fullerenes with square cycles on its surfaces are even more stable than the "classical" ones [19-22]. Four-membered rings are also contained in many recently proposed carbon structures [23-24].

[1] Corresponding author
E-mail: kpkatin@yandex.ru

N.V. Novikov, I.Y. Dolinskiy, M.A. Gimaldinova, K.P. Katin, M.M. Maslov

Boron nitrides form the other promising class of new materials. Both boron and nitrogen atoms are the nearest neighbors to carbon in the Mendeleev's table. For this reason, many carbon architectures have boron nitride analogues, consisted of alternated boron and nitrogen atoms instead of carbon ones. So, boron nitride fullerenes [25], nanotubes [26,27] and other structures [28-30] are actively investigated. Construction of boron nitrides based on already known carbon cages was an efficient way of searching new BN materials. Similar to carbon compounds, some boron nitrides also include four-membered B-N-B-N cycles [31-32].

Most computational studies of novel boron nitrides are based on density functional theory. The commonly used exchange-correlation functionals are B3LYP [33-34] and PBE [35], because they provide high accuracy for many systems [36-37], including boron nitride species [38]. Nevertheless, these functionals were not tested on high-strained boron nitrides with square cycles. For this reason, their application to such untypical systems remains questionable.

In this study, we perform a benchmark study of 24 exchange-correlation functionals on a set of small boron nitride clusters including those with the square cycles. The results, obtained with the density functional theory, were compared with the more accurate data derived from coupled clusters calculations [39-41].

2. Materials and Methods

To test different density functional methods, we chose three boron nitride clusters C_2N_2, C_3N_3 and C_4N_4 with alternated boron and nitrogen atoms. Their structures are presented at Figure 1. Geometries of all three systems were optimized within the density functional and coupled clusters methods until the forces acting on atoms become smaller than 10^{-4} Ha/Bohr. No symmetry constrains were introduces. To confirm that the obtained geometries are true minima on the potential energy hypersurface, we calculate the Hessian matrix at the same level of theory. All considered structures have not any imaginary frequencies and therefore correspond to metastable states.
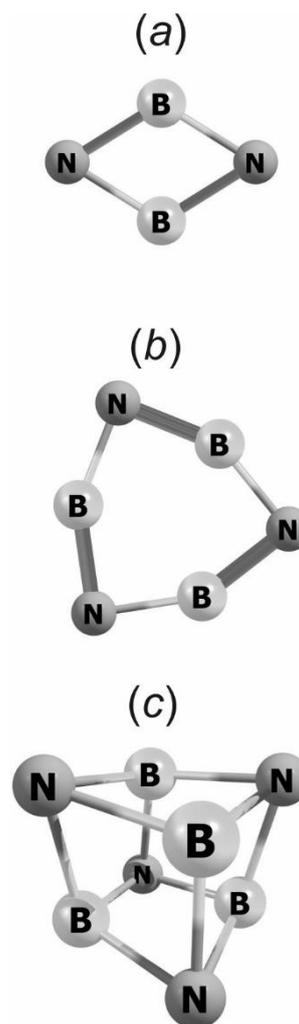

Figure 1. Structures of small boron nitride clusters B_2N_2 (a), B_3N_3 (b) and B_4N_4 (c).

The values of l_{BN}, a_{BNB} and a_{NBN} for each cluster are calculated as the arithmetic means of all B-N bonds lengths, B-N-B and N-B-N angles, respectively (note, that all averaged numbers, corresponding to the same molecule, are almost the same due to the symmetries of the considered systems). The chemical potentials μ are evaluated according to the Koopmans theorem [42] as $\mu = (E_{HOMO} + E_{LUMO})/2$, where E_{HOMO} and E_{LUMO} are the energies of the highest occupied molecular orbital (HOMO) and the lowest unoccupied molecular orbital (LUMO), respectively.

In our density functional calculations, we compare the follow exchange-correlation functionals: B3LYP [33-34], B3LYPV1R [43], B3P86V5 [34], B3PW91 [34], B97 [44], B97-2 [45], B97-3 [46], B97-K [47], CAMB3LYP [48],

N.V. Novikov, I.Y. Dolinskiy, M.A. Gimaldinova, K.P. Katin, M.M. Maslov

LYP [49], M11 [50], OP [49], PBE0 [51], PW91C [52], VWN [53], VWN1RPA [54], wB97 [55-56], wB97X [55-56], wB97X-D [55-56], X3LYP [57], BMK [47], dLDF [58], M05 [59], M06 [60]. The results are compared with the data obtained with the coupled clusters CCSD(T) method [61]. For all calculations, we use the same 6-311G(2d,2p) basic set [62]. Since we restrict our study by the only singlet configurations, the restricted Hartree-Fock method of self-consistent field calculation is applied. All calculations are performed with the GAMESS software [63].

As a measure of difference between geometries, obtained with coupling clusters and density functional methods, we use the value

$$\varepsilon_g = \frac{1}{N} \sum |x_{CC} - x_{DFT}|/x_{CC}. \qquad (1)$$

Here x is one of the geometric parameters (l_{BN}, a_{BNB} or a_{NBN}), N = 9 is the number of terms, summation is performed over all parameters of all considered clusters, indices "CC" and "DFT" correspond to coupled clusters and density functional methods, respectively. A very similar value εε is used as a measure of difference of electronic properties. In this case, x is the chemical potential μ or it means partial Mulliken q_M or Lowdin q_L charge of boron atoms.

3. Results and Discussion

In all three considered boron nitride structures, optimized with the coupled clusters method, all obtained B-N bonds lengths are the same. They are equal to 1.409, 1.363 and 1.511 Å for B_2N_2, B_3N_3 and B_4N_4 clusters, respectively. The value for cubane B_4N_4 (see Figure 1c) slightly differs from the earlier reported coupled clusters results (1.492 [64] and 1.505 Å [65]). However, the authors of Ref. [64] performed only single point calculation of pre-optimized structure, whereas the authors of Ref. [65] applied the CCSD method with symmetry constrains. So, reported here CCSD(T) results are obtained with the higher level of theory and should be regarded as the most accurate.

In Table 1, we present all geometry parameters of considered boron nitride clusters. We can see that the bonds lengths and valence angles, obtained with the density functional methods, differ from the coupled clusters data by ~0.01 Å and ~1°, respectively. The calculated electronic parameters are listed at Table 2. Chemical potentials are compared well with the each other, whereas partial charges demonstrate huge dispersions.

Table 1. Geometric parameters l_{BN} (Å), a_{BNB} and a_{NBN} (degree) of clusters B_2N_2, B_3N_3 and B_4N_4, obtained with the CCSD(T) method. The differences between l_{BN}, a_{BNB} and a_{NBN} values, calculated with the CCSD(T) and DFT approaches, are also listed.

Method	B_2N_2			B_3N_3			B_4N_4		
	l_{BN}	a_{BNB}	a_{NBN}	l_{BN}	a_{BNB}	a_{NBN}	l_{BN}	a_{BNB}	a_{NBN}
CCSD(T)	**1.409**	**63.81**	**116.19**	**1.363**	**88.32**	**151.68**	**1.511**	**75.37**	**102.91**
B3LYP	-0.017	0.46	-0.46	-0.010	0.87	-0.87	-0.010	0.18	-0.14
B3LYPV1R	-0.017	0.46	-0.46	-0.010	0.88	-0.88	-0.010	0.18	-0.14
B3P86V5	-0.015	0.31	-0.31	-0.008	0.03	-0.04	-0.011	-0.13	0.10
B3PW91	-0.016	0.27	-0.27	-0.009	-0.22	0.23	-0.012	-0.26	0.20
B97	-0.012	0.56	-0.57	-0.005	-0.09	0.09	-0.006	0.19	-0.15
B97-2	-0.014	0.15	-0.15	-0.008	-0.36	0.36	-0.012	-0.60	0.46
B97-3	-0.017	0.49	-0.49	-0.010	0.03	-0.03	-0.013	0.01	-0.01
B97-K	-0.013	0.68	-0.68	-0.007	0.37	-0.37	-0.007	0.00	0.00
CAMB3LYP	-0.025	0.71	-0.71	-0.016	1.50	-1.50	-0.018	0.18	-0.14
LYP	-0.045	1.42	-1.42	-0.036	2.87	-2.87	-0.042	0.15	-0.12
M11	-0.019	0.84	-0.84	-0.010	0.86	-0.86	-0.011	-0.78	0.59
OP	-0.042	1.36	-1.36	-0.033	2.58	-2.58	-0.039	0.00	0.00
PBE0	-0.017	0.25	-0.25	-0.228	-0.37	0.37	-0.014	-0.40	0.31
PW91C	-0.044	1.23	-1.23	-0.035	1.94	-1.93	-0.043	-0.25	0.19
VWN	-0.045	1.43	-1.43	-0.036	2.87	-2.86	-0.018	0.19	-0.14
VWN1RPA	-0.047	1.44	-1.44	-0.037	2.80	-2.86	-0.043	0.06	-0.04
wB97	-0.017	0.42	-0.42	-0.008	-0.30	0.30	-0.013	-1.13	0.86
wB97X	-0.020	0.59	-0.59	-0.011	0.27	-0.27	-0.015	-0.53	0.41
wB97X-D	-0.020	0.78	-0.78	-0.011	0.19	-0.18	-0.015	-0.02	0.01

N.V. Novikov, I.Y. Dolinskiy, M.A. Gimaldinova, K.P. Katin, M.M. Maslov

Table 1 continued

X3LYP	-0.018	0.50	-0.50	-0.011	0.98	-0.98	-0.011	0.19	-0.15
BMK	-0.026	1.32	-1.32	-0.015	-0.97	0.97	-0.019	0.15	-0.11
dLDF	-0.014	0.38	-0.38	-0.009	1.62	-1.62	-0.006	-0.95	0.72
M05	-0.017	-0.13	0.13	-0.007	-3.23	3.23	-0.014	-1.89	1.42
M06	-0.022	0.19	-0.19	-0.015	-0.24	0.24	-0.018	-0.67	0.51

Table 2. Chemical potentials μ (eV), mean Mulliken q_M or Lowdin q_L charges of boron atoms (|e|, where e is the elementary charge) of clusters B_2N_2, B_3N_3 and B_4N_4, obtained with the CCSD(T) method. The differences between the values, calculated with the CCSD(T) and DFT approaches, are also listed.

Method	B_2N_2			B_3N_3			B_4N_4		
	μ	q_M	q_L	μ	q_M	q_L	μ	q_M	q_L
CCSD(T)	**-5.73**	**-0.437**	**0.040**	**-5.60**	**-0.275**	**0.128**	**-6.37**	**-0.513**	**0.146**
B3LYP	-0.20	0.144	0.083	-0.21	0.166	0.066	-0.04	0.178	0.081
B3LYPV1R	-0.29	0.143	0.083	-0.30	0.165	0.066	-0.12	0.177	0.081
B3P86V5	-0.39	0.128	0.082	-0.43	0.142	0.069	-0.25	0.157	0.087
B3PW91	-0.29	0.129	0.081	-0.33	0.140	0.069	-0.16	0.155	0.087
B97	-0.18	0.125	0.072	-0.22	0.150	0.064	-0.04	0.158	0.075
B97-2	-0.18	0.139	0.074	-0.19	0.134	0.061	-0.04	0.169	0.083
B97-3	-0.21	0.116	0.070	-0.26	0.141	0.061	-0.10	0.138	0.075
B97-K	-0.17	0.104	0.061	-0.21	0.138	0.057	-0.10	0.135	0.067
CAMB3LYP	-0.39	0.147	0.084	-0.41	0.174	0.066	-0.24	0.185	0.084
LYP	-0.74	0.018	0.024	-0.75	0.032	0.013	-0.73	0.053	0.038
M11	-0.45	-0.014	0.075	-0.56	-0.055	0.059	-0.40	0.043	0.085
OP	-0.62	0.001	0.016	-0.63	0.001	0.006	-0.62	0.027	0.031
PBE0	-0.28	0.141	0.081	-0.34	0.152	0.072	-0.17	0.189	0.092
PW91C	-0.82	0.003	0.021	-0.87	-0.002	0.015	-0.85	0.025	0.045
VWN	-1.13	-0.006	0.010	-1.12	-0.003	-0.004	-1.12	0.021	0.022
VWN1RPA	-1.60	-0.009	0.009	-1.59	-0.004	-0.004	-1.59	0.020	0.022
wB97	-0.28	0.134	0.069	-0.37	0.145	0.059	-0.21	0.165	0.082
wB97X	-0.29	0.130	0.070	-0.36	0.148	0.060	-0.24	0.184	0.088
wB97X-D	-0.26	0.103	0.066	-0.32	0.130	0.059	-0.14	0.118	0.073
X3LYP	-0.25	0.146	0.084	-0.27	0.170	0.067	-0.10	0.845	0.082
BMK	-0.30	0.024	0.054	-0.39	0.135	0.069	-0.20	0.094	0.071
dLDF	-0.66	0.081	0.033	-0.66	0.069	0.008	-0.62	0.099	0.033
M05	-0.13	0.120	0.066	-0.28	0.171	0.066	-0.04	0.124	0.086
M06	-0.27	0.074	0.068	-0.33	0.095	0.053	-0.13	0.038	0.074

The mean geometry and electronic errors (ε_g and ε_e), calculated with different exchange-corrected functionals using formula (1), are collected at Table 3. We conclude that B3P86V5 and B97 functionals reproduce well the geometries, whereas the OP and VWN provide the best matches of electronic properties. OP and VWN functionals also provide the minimal values of $\varepsilon_g + \varepsilon_e$. Using of popular B3LYP and PBE0 functionals results in higher errors εg and εe.

N.V. Novikov, I.Y. Dolinskiy, M.A. Gimaldinova, K.P. Katin, M.M. Maslov

Table 3. The values of mean errors ε_g and ε_e for different exchange-corrected functionals (see formula (1) for details). The sums of two errors are also presented.

functional	ε_g	ε_e	$\varepsilon_g + \varepsilon_e$
B3LYP	0.0063	0.5003	0.5066
B3LYPV1R	0.0063	0.5045	0.5108
B3P86V5	**0.0038**	0.4981	0.5019
B3PW91	0.0047	0.4892	0.4939
B97	**0.0039**	0.4476	0.4515
B97-2	0.0051	0.4558	0.4609
B97-3	0.0045	0.4319	0.4364
B97-K	0.0047	0.3905	0.3952
CAMB3LYP	0.0099	0.5224	0.5323
LYP	0.0195	0.1777	0.1972
M11	0.0089	0.3862	0.3951
OP	0.0177	**0.1151**	**0.1328**
PBE0	0.0233	0.5108	0.5341
PW91C	0.0172	0.1605	0.1777
VWN	0.0178	**0.1190**	**0.1368**
VWN1RPA	0.0196	0.1438	0.1634
wB97	0.0073	0.4501	0.4574
wB97X	0.0069	0.4631	0.4700
wB97X-D	0.0061	0.4082	0.4143
X3LYP	0.0069	0.6547	0.6616
BMK	0.0105	0.3620	0.3725
dLDF	0.0087	0.2304	0.2391
M05	0.0140	0.4413	0.4553
M06	0.0068	0.3708	0.3776

4. Conclusion

In the study presented, we perform a comparable analysis of density functional approaches applied to the small boron nitride clusters. The data obtained provide a reasonable choice of the most suitable exchange-corrected DFT-functional for strained BN-systems numerical simulation. We consider that the reported results stimulate further density functional studies not only of pristine boron nitrides, but also of their strained analogues such as prismanes, non-classical fullerenes, and silicic cages both in molecular and crystalline forms.

References

[1] M. Monthioux, Filling single-wall carbon nanotubes, Carbon 40 (2002) 1809–1823.

[2] W. Krätschmer, D. R. Huffman, Fullerites: New forms of crystalline carbon, Carbon 30 (1992) 1143–1147.

[3] E. A. Belenkov, V. A. Greshnyakov, New structural modifications of diamond: LA9, LA10, and CA12, Journal of Experimental and Theoretical Physics 119 (2014) 101–106.

[4] V. A. Greshnyakov, E. A. Belenkov, Structures of diamond-like phases, Journal of Experimental and Theoretical Physics 113 (2011) 86–95.

[5] Y. A. Kvashnina, A. G. Kvashnin, P. B. Sorokin, Investigation of new superhard carbon allotropes with promising electronic properties, Journal of Applied Physics 114 (2013) 183708.

[6] Yu. A. Kvashnina, A. G. Kvashnin, M. Yu. Popov, B. A. Kulnitskiy, I. A. Perezhogin, E. V. Tyukalova, L. A. Chernozatonskii, P. B. Sorokin, V. D. Blank, Toward the Ultra-incompressible Carbon Materials. Computational Simulation and Experimental Observation, Journal of Physical Chemistry Letters 6 (2015) 2147–2152.

[7] R. A. Brazhe, A. A. Karenin, A. I. Kochaev, R. M. Meftakhutdinov, Elastic characteristics of 2D carbon supracrystals as compared to graphene, Physics of the Solid State 53 (2011) 1481–1483.

[8] R. A. Brazhe, A. I. Kochaev, V. S. Nefedov, Young's modulus and the Poisson's ratio of planar and nanotubular supracrystalline structures, Physics of the Solid State 54 (2012) 1430–1432.

[9] G. Maier, S. Pfriem, U. Schäfer, R. Matusch, Tetra-tert-butyltetrahedrane, Angewandte Chemie International Edition 17 (1978) 520–521.

[10] G. Maier, D. Born, Tri-tert-butyl(trimethylsilyl)tricyclo[1.1.0.02, 4]-butane–a Second Tetrahedrane Derivative, Angewandte Chemie International Edition 28 (1989) 1050–1052.

[11] T. J. Katz, N. Acton, Synthesis of prismane, Journal of the American Chemical Society 95 (1973) 2738–2739.

[12] P. E. Eaton, T. W. Cole, Cubane, Journal of the American Chemical Society 86 (1964) 3157–3158.

[13] P. E. Eaton, Cubanes: Starting Materials for the Chemistry of the 1990s and the New Century, Angewandte Chemie International Edition 31 (1992) 1421–1436.

[14] K. A. Lukin, J. Li, P. E. Eaton, N. Kanomata, J. Hain, E. Punzalan, R. Gilardi, Synthesis and chemistry of 1,3,5,7-tetranitrocubane including measurement of its acidity,

formation of o-nitro anions, and the first preparations of pentanitrocubane and hexanitrocubane, Journal of the American Chemical Society 119 (1997) 9591–9602.

[15] M. X. Zhang, P. E. Eaton, R. Gilardi, Hepta- and octanitrocubanes, Angewandte Chemie International Edition39 (2000) 401–404.

[16] P. E. Eaton, M. X. Zhang, R. Gilardi, N. Gelber, S. Iyer, R. Surapaneni, Octanitrocubane: A new nitrocarbon, Propellants, Explosives, Pyrotechnics 27 (2002) 1–6.

[17] P. E. Eaton, Y. S. Or, S. J. Branca, Pentaprismane, Journal of the American Chemical Society 103 (1981) 2134–2136.

[18] F. Pichierri, Hypercubane: DFT-based prediction of an Oh-symmetric double-shell hydrocarbon, Chemical Physics Letters 612 (2014) 198–202.

[19] C. Killblane, Y. Gao, N. Shao, X. C. Zeng, Search for Lowest-Energy Nonclassical Fullerenes III: C22, Journal of Physical Chemistry A 113 (2009) 8839–8844.

[20] W. An, N. Shao, S. Bulusu, X. C. Zeng, Ab initio calculation of carbon clusters. II. Relative stabilities of fullerene and nonfullerene C24, Journal of Chemical Physics 128 (2008) 084301.

[21] J. An, L. H. Gan, J. Q. Zhao, R. Li, A global search for the lowest energy isomer of C26, Journal of Chemical Physics 132 (2010) 154304.

[22] W. W. Wang, J. S. Dang, X. Zhao, Impact of tetragonal rings on the stability of small fullerenes encapsulated with noble gas: A density functional theory survey, Chemical Physics Letters 536 (2012) 77–81.

[23] Y. A. Kvashnina, D. G. Kvashnin, A. G. Kvashnin, P. B. Sorokin, New allotropic forms of carbon based on C60 and C20 fullerenes with specific mechanical characteristics, JETP Letters 105 (2017) 419–425.

[24] D. S. Lisovenko, J. A. Baimova, L. K. Rysaeva, V. A. Gorodtsov, A. I. Rudskoy, S. V. Dmitriev, Equilibrium diamond-like carbon nanostructures with cubic anisotropy: Elastic properties, Physica Status Solidi B 253 (2016) 1295–1302.

[25] X. Xia, D. A. Jelski, J. R. Bowser, T. F. George, MNDO Study of Boron-Nitrogen Analogs of Buckminsterfullerene, Journal of the American Chemical Society 114 (1992) 6493–6496.

[26] E. J. Hamilton, S. E. Dolan, C. M. Mann, H. O. Colijn, C. a McDonald, S. G. Shore, Preparation of amorphous boron nitride and its conversion to a turbostratic, tubular form, Science 260 (1993) 659–661.

[27] A. Loiseau, F. Willaime, N. Demoncy, G. Hug, H. Pascard, Boron Nitride Nanotubes with Reduced Numbers of Layers Synthesized by Arc Discharge, Physical Review Letters 76 (1996) 4737–4740.

[28] L. Bourgeois, Y. Bando, S. Shinozaki, K. Kurashima, T. Sato, Boron nitride cones: structure determination by transmission electron microscopy, Acta Crystallographica A 55 (1999) 168–177.

[29] L. Bourgeois, Y. Bando, W. Han, T. Sato, Structure of boron nitride nanoscale cones: Ordered stacking of 240° and 300° disclinations, Physical Review B 61 (2000) 7686–7691.

[30] K. Terauchi, M., Tanaka, M., Suzuki, K., Ogino, A., Kimura, Nanotubes, Production of zigzag-type BN Annealing, and BN cones by thermal, Chemical Physics Letters 324 (2000) 359–364.

[31] M. T. Baei, H. Mohammadian, S. Hashemian, B12N12 nanocage as a potential adsorbent for the removal of aniline from environmental systems, Bulgarian Chemical Communications 46 (2014) 735–742.

[32] M. D. Esrafili, S. Chashmniam, V. Alizadeh, A DFT Study of Hydrogen Adsorption on Ln@B16N16 Fullerene-Like Nanocage (Ln: La, Gd and Lu), Fullerenes, Nanotubes and Carbon Nanostructures 22 (2014) 928–937.

[33] C. Lee, W. Yang, R. G. Parr, Development of the Colle-Salvetti correlation-energy formula into a functional of the electron density, Physical Review B 37 (1988) 785–789.

[34] A. D. Becke, Density-functional thermochemistry. III. The role of exact exchange, Journal of Chemical Physics 98 (1993) 5648–5652.

[35] J. P. Perdew, K. Burke, M. Ernzerhof, Generalized Gradient Approximation Made

Simple, Physical Review Letters 77 (1996) 3865–3868.

[36] J. G. Brandenburg, T. Maas, S. Grimme, Benchmarking DFT and semiempirical methods on structures and lattice energies for ten ice polymorphs, Journal of Chemical Physics 142 (2015) 124104.

[37] É. Brémond, M. Savarese, N. Q. Su, Á. J. Pérez-Jiménez, X. Xu, J. C. Sancho-García, C. Adamo, Benchmarking Density Functionals on Structural Parameters of Small-/Medium-Sized Organic Molecules, Journal of Chemical Theory and Computation 12 (2016) 459–465.

[38] D. Karakas, Theoretical investigation on electrophilicity indexes and proton affinities of some boron-nitrogen open-chain species, Turkish Computational and Theoretical Chemistry 1 (2017) 1–10.

[39] K. Raghavachari, G. W. Trucks, J. A. Pople, M. Head-Gordon, Reprint of: A fifth-order perturbation comparison of electron correlation theories, Chemical Physics Letters 589 (2013) 37–40.

[40] H. J. Monkhorst, Calculation of properties with the coupled-cluster method, International Journal of Quantum Chemistry 12 (1977) 421–432.

[41] P. Piecuch, S. A. Kucharski, K. Kowalski, M. Musiał, Efficient computer implementation of the renormalized coupled-cluster methods: The R-CCSD[T], R-CCSD(T), CR-CCSD[T], and CR-CCSD(T) approaches, Computer Physics Communications 149 (2002) 71–96.

[42] T. Koopmans, Über die Zuordnung von Wellenfunktionen und Eigenwerten zu den Einzelnen Elektronen Eines Atoms, Physica 1 (1934) 104–113.

[43] P. J. Stephens, F. J. Devlin, C. F. Chabalowski, M. J. Frisch, Ab initio calculation of vibrational absorption and circular dichroism spectra using density functional force fields, Journal of Chemical Physics 98 (1994) 11623–11627.

[44] A. D. Becke, Density-functional thermochemistry. V. Systematic optimization of exchange-correlation functionals, Journal of Chemical Physics 107 (1997) 8554-8560.

[45] P. J. Wilson, T. J. Bradley, D. J. Tozer, Hybrid exchange-correlation functional determined from thermochemical data and ab initio potentials, Journal of Chemical Physics 115 (2001) 9233-9242.

[46] T. W. Keal, D. J. Tozer, Semiempirical hybrid functional with improved performance in an extensive chemical assessment, Journal of Chemical Physics 123 (2005) 121103.

[47] A. D. Boese, J. M. L. Martin, Development of density functionals for thermochemical kinetics, Journal of Chemical Physics 121 (2004) 3405-3416.

[48] T. Yanai, D. P. Tew, N. C. Handy, A new hybrid exchange–correlation functional using the Coulomb-attenuating method (CAM-B3LYP), Chemical Physics Letters 393 (2004) 51–57.

[49] T. Tsuneda, K. Hirao, A new spin-polarized Colle-Salvetti-type correlation energy functional, Chemical Physics Letters 268 (1997) 510-520.

[50] R. Peverati, D. G. Truhlar, Improving the accuracy of hybrid meta-GGA density functionals by range separation, Journal of Physical Chemistry Letters 2 (2011) 2810-2817.

[51] C. Adamo, V. Barone, Toward reliable density functional methods without adjustable parameters: The PBE0 model, Journal of Chemical Physics 110 (1999) 6158-6170.

[52] J. P. Perdew, Y. Wang, Accurate and simple analytic representation of the electron gas correlation energy, Physical Review B 45 (1992) 13244–13249.

[53] S. H. Vosko, L. Wilk, M. Nusair, Accurate spin-dependent electron liquid correlation energies for local spin density calculations: a critical analysis, Canadian Journal of Physics 58 (1980) 1200-1211.

[54] P. Salek, A. Hesselmann, A self-contained and portable density functional theory library for use in Ab Initio quantum chemistry programs, Journal of Computational Chemistry 28 (2007) 2569-2575.

[55] J. D. Chai, M. Head-Gordon, Systematic optimization of long-range corrected hybrid density functionals, Journal of Chemical Physics 128 (2008) 084106.

[56] J. D. Chai, M. Head-Gordon, Long-range corrected hybrid density functionals with damped atom–atom dispersion corrections,

N.V. Novikov, I.Y. Dolinskiy, M.A. Gimaldinova, K.P. Katin, M.M. Maslov

Physical Chemistry Chemical Physics 10 (2008) 6615-6620.

[57] X. Xu, Q. Zhang, R. P. Muller, W. A. Goddard, An extended hybrid density functional (X3LYP) with improved descriptions of nonbond interactions and thermodynamic properties of molecular systems, Journal of Chemical Physics 122 (2005) 014105.

[58] K. Pernal, R. Podeszwa, K. Patkowski, K. Szalewicz, Dispersionless Density Functional Theory, Physical Review Letters 103 (2009) 263201.

[59] Y. Zhao, N. E. Schultz, D. G. Truhlar, Exchange-correlation functional with broad accuracy for metallic and nonmetallic compounds, kinetics, and noncovalent interactions, Journal of Chemical Physics 123 (2005) 161103.

[60] Y. Zhao, D.G. Truhlar, The M06 suite of density functionals for main group thermochemistry, thermochemical kinetics, noncovalent interactions, excited states, and transition elements: two new functionals and systematic testing of four M06-class functionals and 12 other functionals, Theoretical Chemistry Accounts 120 (2007) 215-241.

[61] T. Helgaker, P. Jorgensen, J. Olsen. Molecular Electronic-Structure Theory. Wiley: New York, 2000, 793-796.

[62] R. Krishnan, J. S. Binkley, R. Seeger, J. A. Pople, Self-consistent molecular orbital methods. XX. A basis set for correlated wave functions, Journal of Chemical Physics 72 (1980) 650–654.

[63] M. W. Schmidt, K. K. Baldridge, J. A. Boatz, S. T. Elbert, M. S. Gordon, J. H. Jensen, S. Koseki, N. Matsunaga, K. A. Nguyen, S. Su, T. L. Windus, M. Dupuis, J. A. Montgomery Jr, General atomic and molecular electronic structure system, Journal of Computational Chemistry 14 (1993) 1347–1363.

[64] F. Jensen, The stability of cage and ring isomers for carbon and boron nitride clusters, Chemical Physics Letters 209 (1993) 417–422.

[65] M. R. Manaa, A comparative study of cubic B4N4 and C8, Journal of Molecular Structure: THEOCHEM 549 (2001) 23–26.